Heliyon 10 (2024) e28714

Contents lists available at ScienceDirect

Heliyon

journal homepage: www.cell.com/heliyon

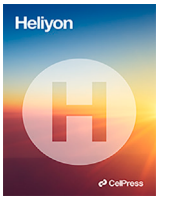

Research article

Four port tri-circular ring MIMO antenna with wide-band characteristics for future 5G and mmWave applications

Mehr E. Munir *, Moustafa M. Nasralla, Maged Abdullah Esmail

Smart Systems Engineering Lab, Department of Communications and Networks Engineering, Prince Sultan University Riyadh, 145111, Saudi Arabia

ARTICLE INFO

Keywords:
Four elements
mmWave
MIMO system
28 GHz
38 GHz
Wideband
Gain
Efficiency

ABSTRACT

MIMO (Multiple-Input-Multiple-Output) antenna systems are promising for fifth-generation (5G) networks, offering lower latency and higher data rates. These systems utilize millimeter-wave (mmWave) frequency bands for efficient transmission and reception of multiple data simultaneously, enhancing overall efficiency and performance. This article presents a compact size, wide band tri-circular ring mmWave MIMO antenna with suitable performance characteristics for next-generation communication systems. The MIMO system consists of a tri-circular ring patch with slots on a ground plane. The four elements of the antenna are arranged together in the polarization diversity configuration with overall dimensions of 23×18×0.254 mm^3, and designed on a 0.254 mm thin, flexible RO5880 substrate with a relative permittivity of 2.3 using Computer Simulation Technology (CST) 2022. The proposed antenna design shows the impedance bandwidth of 14 GHz with isolation >18 dB throughout the 26-40 GHz resonance band. The obtained gain is 6.6 dBi at 28 GHz with radiation efficiency > 90%. Several MIMO parameters are also investigated, such as Envelope Correlation Coefficient (ECC), Mean Effective Gain (MEG), Diversity Gain (DG), Total Active Reflection Co-efficient (TARC), and Channel Capacity Loss (CCL), and are found to be within the accepted limits for a practical MIMO system. Furthermore, the fabricated MIMO antenna was tested, and the measured results aligned favorably with the simulated results, confirming the suitability of the proposed design. Through the obtained results, the mmWave MIMO antenna is suitable for practical 5G as well as mmWave applications due to its lightweight, simple design, and wideband characteristics, which cover the 5G frequency bands of 26, 28, 32, and 38 GHz.

1. Introduction

Antenna engineering has gained significant popularity due to its wide-ranging applications in several fields, such as remote sensing, imaging, defense systems, satellite communication, healthcare areas, wireless communication, and radio frequency identification (RFID) tags. The exponential growth in mobile data consumption and the widespread adoption of smart devices pose significant issues for wireless service providers in addressing a global scarcity of bandwidth. Recently, mobile network operators are making efforts to offer high-quality video and multimedia apps with minimal buffering to mobile customers. However, such efforts are constrained by a carrier frequency range that ranges from 700 MHz to 2.6 GHz. Mobile network providers are restricted from utilizing frequencies within this range for their communication services. They are allocated a certain bandwidth within this frequency range to transmit

* Corresponding author.
E-mail addresses: mmunir@psu.edu.sa (M.E. Munir), mnasralla@psu.edu.sa (M.M. Nasralla), mesmail@psu.edu.sa (M.A. Esmail).

https://doi.org/10.1016/j.heliyon.2024.e28714
Received 21 January 2024; Received in revised form 17 March 2024; Accepted 22 March 2024

Available online 5 April 2024

and receive the signals [1]. Advanced technology in 5G wireless communication systems offers increased data capacity, low latency, and improved system reliability. This technology surpasses predecessors like 4G and 3G in bandwidth and beam-forming capabilities. Current antenna systems lack infrastructure for real-time video streaming, cloud storage, and social applications, requiring access to significantly more data simultaneously. Applications like real-time video streaming require a significant amount of data to be transmitted and received continuously to ensure smooth playback and seamless user experience. Similarly, cloud storage and social applications involve the transfer of large volumes of data, such as files, photos, and videos, between users and remote servers [2].

Wireless communication has been given a new direction to Multiple-Input-Multiple-Output (MIMO) antennas, and these antennas have become particularly desirable for use in 5G applications. In the current environment, developing a small MIMO antenna for 5G networks is an extremely difficult task. MIMO antennas are initially used to enhance spatial diversity as an approach to mitigate the effects of channel fading. The data is being evaluated within the framework of a Rayleigh fading environment, where it is transmitted by antennas that follow distinct paths to autonomously reach the receiving antenna. In this scenario, there is an increase in the highest possible diversity, which is known as spatial diversity. Spatial multiplexing refers to the technique of increasing the transmission rate by transmitting different information through multiple antennas. In the scenario of MIMO antennas, it is essential to minimize both mutual coupling loss and correlation coefficient between the antennas. The upgraded MIMO antenna specifications for the 5G wireless communication networks have been officially released by the 3rd Generation Partnership Project (3GPP) in its seventeenth version [3]. The primary areas of emphasis for 3GPPP encompass several key aspects. These include the investigation of multi-beam formation techniques, the provision of extra-terrestrial coverage below 7 GHz, the enhancement of efficiency through antenna tuning systems in mobile devices, the expansion of spectrum allocation from 24.25 to 52.6 GHz, extending up to 71 GHz, the optimization of bandwidth allocation to support Internet of Things (IoT) devices at 20 MHz/100 MHz in emerging Sub-7 GHz/mmWave frequencies, and the development of mobile MIMO antenna systems [4]. The basic principle of MIMO technology is to use multiple antennas to transmit and receive signals simultaneously, which can increase the data rate and improve the reliability of the communication system. In a four-port MIMO mmWave 5G antenna system, four elements are connected to four transceivers, which can transmit and receive signals independently. These mmWave MIMO 5G systems are typically designed to have a directional radiation pattern, which means that they can transmit and receive signals in a specific direction. This is attained by designing the shape and size of the antenna to control the direction of the electromagnetic wave. During the transmission, each element in the four-port 5G system transmits a signal simultaneously, which can be combined at the receiver to increase the data rate and improve the reliability of the communication system. This is achieved by utilizing signal processing techniques, such as spatial multiplexing, which separates the signals transmitted by each antenna and combines them at the receiver to increase the data rate. During reception, each antenna in the four-port MIMO 5G system receives a signal simultaneously, which can be combined at the receiver to improve the quality of the received signal. This is achieved by using beam-forming techniques, which focus on the received signals in a specific direction to improve the signal-to-noise ratio [5].

5G-powered systems facilitate the use of compact devices and achieve high data transfer speeds by utilizing wider bandwidth and lower latency. The standards provide data rates of up to 1 Gigabit, ensuring minimal delay along the communication path. As the demand for communication facilities grows, academic research institutes and commercial appliance makers focus on 5G technology for new call management solutions. Data transmission speeds have increased with each new iteration of communication technologies, which has also introduced improved connection quality and unique services. The currently used 4G technology was commercially deployed in 2009. 4G technology has revolutionized mobile telecommunications, offering faster data rates, enhanced network capacity, and superior performance. Widely adopted globally, it provides seamless experiences for data-intensive applications like internet browsing, video streaming, and online gaming. [6]. The 5G system includes several new facilities, such as the concept of smart cities and those related to the IoT. The installation of a broad 5G network requires the establishment of antenna infrastructure and the implementation of novel technical specifications. One potential approach for installing 5G-enabled devices is the incorporation of highly directional antennas that fulfill the requirements for a 5G wireless network [7]. The Sub-6 GHz region and the mmWave region are the two categories that are used to classify 5G technologies. It has been determined that the mmWave band is a more promising and possible candidate for use in upcoming cellular devices. The mmWave band, which covers the starting frequency of 24 GHz and above, can be utilized for future 5G networks [8]. The mmWave spectrum is well-known for its capacity to provide high transmission rates in the multi-gigabit per second range and offers an increased bandwidth allocation to meet the requirements of 5G networks. The International Telecommunications Union (ITU) has allocated the frequency bands centered at 26, 28, 32, 38, 60, and 73 GHz for the allocation of 5G mobile networks. These frequency bands are currently unlicensed and can be used without any restrictions [9].

The paper layout is organized as follows: Section 1 covers the introduction of the 5G antenna. Section 2 discusses the literature review of previously published techniques related to the research work. Section 3 focuses on the single-element antenna design. Section 4 explains the MIMO antenna configuration. Section 5 reports the results with a discussion of antenna design. Section 6 explores the MIMO performance parameters and a compression table of obtained results with previously published research. Finally, Section 7 concludes the research work.

2. Related work

The antenna that is designed specifically for wireless networks is responsible for transmitting or receiving power based on the spatial parameters that have been defined for a particular network. Each particular network is responsible for transmitting or receiving the signal to the specific user location. The optimization and commercialization of 5G communication devices in mmWave is a challenging task due to the smaller wavelength and the need for point-to-point communication. Highly directional antennas are

desired for effective communication services in the mmWave region, ensuring efficient and effective communication for individual or group users. [10]. Several designs in [11], [12], [13], [14], [15], [16], [17], [18], [19], [20], [21], [22], [23], [24], [25], [26], [27] and [28] have been presented; each design addresses the issues and challenges efficiently. In [11], a compact antenna is presented with minimum transmission line losses. The physical length of the antenna design is 28.8×28.8 mm^2, with a 57-71 GHz frequency range and a maximum gain of 26.7 dBi, due to the employing bonding films and the inclusion of a multi-layer substrate, this antenna's design configuration is quite complicated. Moreover, the assembly of this antenna is exceptionally challenging. A dual-band response is established in a four-port planar MIMO antenna array at mmWave bands such as 27.6 GHz and 38.6 GHz is noted with a gain of 7.1 and 7.9 dBi [12]. The assembly of the proposed antenna system is simple. However, the bandwidth response reported in the proposed literature is too low for practical use in 5G services. The authors have introduced a four-port MIMO system in [13] that uses an arc-shaped design to achieve wideband characteristics. The MIMO antenna exhibits a gain of 12 dB, which is considered beneficial and reliable for 5G applications. The MIMO antenna, designed for mmWave systems, measures 80×80 mm^2, making it suitable for practical use. However, the proposed orthogonal MIMO assembly does not display pattern diversity characteristics. In [14], a four-port antenna is introduced for future mobile phone applications in the mmWave frequency range. The resonance frequency of the proposed antenna ranged from 27.5 to 40 GHz. The antenna exhibited a peak gain of 7.2 dB and an isolation level of -17 dB. However, regarding user mobile terminals, the radiation efficiency was measured at 65% at a frequency of 28 GHz, which is insufficient for practical applications.

Similarly, in [15], the proposed metamaterial dual band antenna, operating at sub6GHz and mmWave regions, offers good performance when integrated with a single negative (SNG) metamaterial. It is helpful in mmWave and Sub-6 GHz applications, but artificially constructed metamaterials increase fabrication complexity and system cost. Furthermore, the SIW array is presented in [16] with dimensions of 70×63.5 mm^2. The covering frequency of the antenna is 27.3-29.6 GHz with a radiation efficiency of 60%. Due to its large size and low radiation efficiency, the antenna isn't appropriate for a useful smart mobile device. Similarly, in [17], a SIW array antenna was introduced with a total size of 45×20 mm^2. The antenna's planned operational frequency ranges from 25.05- 34.92 GHz, exhibiting a significant gain of 12.15 dBi and a radiation efficiency above 85% across the whole bandwidth. Despite the good performance of the SIW array in terms of narrow beam width, it is interesting to note that the vias assemblies exhibit a compactness issue, which makes it difficult to use this prototype for practical applications. Furthermore, the complex geometry of the structure, characterized by a high density of vias in close proximity, contributes to the increased complexity of the SIW antenna. A MIMO infinity-shaped antenna was designed in [18] for future 5G devices. The proposed antenna is suitable for mmWave devices operating at a frequency range of 27-30 GHz. It has a maximum gain of 6.1 dBi, and the ECC is below 0.16. However, the antenna system exhibits a relatively lower gain when applied to MIMO systems. The authors of [19] offered a MIMO system that operates at both 4G and 5G frequencies. The proposed work covered the Global System for Mobile Communications (GSM)/Universal Mobile Telecommunications System (UMTS) spectrum for 4G and the Sub6GHz frequency for 5G applications. A massive MIMO array designed for 5G devices was proposed in [20]. The designs cover only the lower frequency bands, resulting in a comparatively lower gain and isolation. Specifically, in the 4G and 5G bands, the antenna achieves peak gains of 4 dBi and 8 dBi, respectively. However, no specific solution is proposed for 5G MIMO applications. Furthermore, the research presented in [21] also offers commendable performance characteristics, including high gain and broad bandwidth, specifically catering to the desired frequencies of both 4G and 5G. However, it is worth noting that the investigation of MIMO configuration is not included in the 4G and 5G designs proposed in the study. Similarly, in [22], the mmWave band antenna achieved a high gain of 7 dBi. However, the suggested approach has significant errors, including insufficient information on gain and radiation efficiency for the lower band. Moreover, there is no proposed solution for MIMO applications. Dielectric Resonator Antenna (DRA) is presented in [23] and [24] with a limited data rate of approximately 1 GHz for 5G applications. The proposed antenna is based on the SIW technique with a maximum gain of 7.73 dBi.

A reflector-based antenna system on Electromagnetic Band-Gap (EBG) offered a wide bandwidth band of 20-33 GHz with a high gain of 11.5 dBi. The evaluation of the suggested MIMO system focused solely on the ECC and diversity gain (DG). The antenna's complicated structure renders it unsuitable for practical implementation in devices supporting 5G. Moreover, in [25], a nature-inspired MIMO antenna is introduced for 5G technologies. The antenna operates within a frequency range of 26-30 GHz, with a central frequency of 28 GHz. It exhibits a narrow bandwidth of 4 GHz. The physical dimensions of the antenna are 30×30 mm^2, and it achieves an Envelope Correlation Coefficient (ECC) of less than 0.2. In [27], the author introduces a MIMO system designed specifically for upcoming 5G devices. The proposed design operates within a 24-39 GHz frequency range and achieves a peak gain of 7.1 dBi. The antenna has compact dimensions, measuring 24x24 mm, and exhibits a high total antenna efficiency of 92%. The ECC is impressively maintained below 0.001, indicating minimal correlation between the antenna elements. To enhance isolation and reduce mutual coupling among the radiating elements, an isolating structure is introduced, and the proposed MIMO antenna elements are arranged orthogonally to one another. A four-element MIMO antenna was presented in [28] using a defective ground structure for 5G mmWave applications. The proposed antenna size is 30 ×35 mm^2 with an operating frequency range of 25.5–29.6 GHz. The maximum gain achieved by the antenna is 8 dBi with a total efficiency of 80%. Furthermore, the ECC was evaluated in order to measure the MIMO capability of the suggested antenna system. A new design for a compact MIMO antenna has been developed to enhance gain across a wide bandwidth [29]. The antenna consists of two identical elements, spaced at half a wavelength, and uses a Y-shaped power divider to feed two modified Vivaldi radiators. A square-ring unit cell metasurface and a U-shaped slot are incorporated to optimize performance. The prototype has an impressive impedance bandwidth of 11.5 to 21.3 GHz with a total antenna size of 36 × 33 × 20 mm^3, isolation of ≥24.92 dB, maximum gain of 10.6 dBi, and radiation efficiency ranging from 88.01% to 90.02%. The antenna's potential applications in frequency-modulated continuous wave (FMCW) radar sensors have been

demonstrated through successful experiments on human subjects. However, due to its larger size, it is not suitable for portable 5G devices like smartphones.

The authors present a dual-polarized MIMO Vivaldi antenna for intelligent Internet of Vehicles (IoV) wireless communications [30]. The antenna consists of four identical orthogonally-crossed vivaldi radiators, a crossed-fishbone-shaped slot, a metasurface lens, parasitic stubs, an electromagnetic wave reflector, and a three-dimensional (3D) printed radome housing a dielectric resonator (DR) array. The antenna's performance is optimized by minimizing inter-element mutual coupling and amplifying gain through the metasurface lens, parasitic stubs, and DR array. Integrating an EM wave reflector enhances boresight gain and mitigates the influence of the vehicle's body on antenna performance. The antenna's diversity performance shows improved MIMO capability, and the impact of weather conditions is thoroughly investigated. The proposed antenna strongly agrees with measured and simulated results, with an impedance bandwidth of 7.55 to 22.85 GHz and port isolation of 18.05 dB with a total antenna size of 138.2 × 69.6 × 31.7 mm^3. The antenna's radiation efficiency ranges from 85.05% to 90.27%, demonstrating its potential for various wireless applications, especially in IoV. However, the larger antenna size makes it unsuitable for portable 5G devices like smartphones.

The eight-element MIMO antenna designed for 5G terminals with a total antenna size of 50 × 3 mm^2, operating in the sub-6 GHz band of 3.4 -3.6 GHz [31]. The antenna is a loop type connected through a 50 micro-strip line and mounted on side-frames. It achieves an isolation of 14.8 dB at the operating frequency and at least 62% efficiency for all antennas. The array has a low ECC of less than 0.1, indicating minimal correlation between antenna elements and excellent MIMO performance. However, the antenna targets the sub-6 GHz frequency band with a narrow impedance bandwidth of 0.2 GHz. A coplanar waveguide (CPW) 1×4 array antenna was presented in [32]. The antenna was developed for 28 GHz and 38 GHz applications. The antenna covered the frequencies from 27.5 GHz to 30.9 GHz and from 37.3 GHz to 44.6 GHz, with peak gains of 5.7 dBi and 6.28 dBi, respectively, having a total antenna size of 40.4 × 20 mm^2. It is important to note that the optimal number of antenna elements in a system depends on several factors, including the specific application, desired data rates, system requirements, and deployment constraints. As technology advances and communication requirements evolve, the number of antenna elements in next-generation communication systems will likely increase. However, a four-element antenna system can still offer valuable benefits and be a practical solution in certain situations. 1) In the early stages of deploying next-generation communication systems, such as 5G, starting with a smaller number of antenna elements may be more practical. This allows more straightforward implementation and compatibility with existing infrastructure while providing improved performance compared to previous generations. As the technology matures and evolves, the number of antenna elements can be increased to meet growing demands. 2) A four-element antenna system can provide diversity reception, where multiple antennas receive the same signal from different spatial paths. This helps combat fading and improves the reliability of the received signal. Diversity techniques mitigate the effects of multipath propagation, ensuring more consistent and robust communication, especially in challenging environments. 3) While higher data rates may necessitate a more significant number of antenna elements, there are scenarios where a four-element antenna system can provide a compact and cost-effective solution. For example, in portable devices with limited space or applications where cost constraints are a significant factor, a four-element antenna system can balance performance and practicality.

This work presents a tri-circular ring shape, wideband four-element MIMO system design for mmWave communication systems. The polarization diversity method is used in the proposed design with an overall size of 23×18×0.254 mm^3, which can easily be used in portable communication systems. The wide band response is achieved by using a defected ground structure (DGS) technique. The MIMO antenna operates in the range of 26-40 GHz with wide-band characteristics of 14 GHz. This antenna offers various remarkable characteristics, such as increased gain, improved radiation efficiency, enhanced isolation, improved diversity performance, and compact size compared to antennas mentioned in the current literature. The proposed MIMO system has wide-band features that cover the four mmWave 5G allocated frequencies of 26, 28, 32, and 38 GHz. The main goal of this antenna design is to provide a compact solution that is easy to fabricate, making it well-suited for portable 5G devices requiring compact antennas.

3. Antenna design (single element)

The mmWave antenna was developed using Computer Simulation Technology (CST) 2022, microwave studio, to design and fabricate it on an ultra-thin RO5880 substrate with a thickness of 0.254 mm and a relative permittivity of 2.3. The antenna design incorporates tri-circular rings on the patch, along with a square slot located at the top middle section of the ground plane, which contributes to achieving the desired bandwidth, as illustrated in Fig. 1. Fig. 1a presents the front view of the antenna, while Fig. 1b displays the ground view. The overall dimensions of the antenna are 7×11×0.254 mm^3. The Anritsu Shock Line MS46122B Vector Network Analyzer (VNA) is used to measure the S-parameter response, revealing that the reflection coefficient response of a single element matched the measured response, as shown in Fig. 1c. The antenna demonstrated an operating band with an overall efficiency exceeding 89%, along with a peak gain of 3.8 dBi and 5.36 dBi at 28 GHz and 38 GHz, respectively, as displayed in Fig. 1d, while the comparison between the simulated (Sim) and measured (Mea) results of Gain over frequency can be observed in Fig. 1e. Fig. 1f–g depicts the radiation pattern in the principal planes, specifically the zx plane $\Phi = 0°$ and zy plane $\Phi = 90°$. In the zx plane, the main lobe is oriented at 0°, exhibiting a 3 dB angular width of 139°, and in the xy plane, the main lobe exhibits a slight tilt towards 358°, while the side lobe level measures -1.3. The simulated and measured outcomes of the single-element antenna align well with the requirements for 5G mmWave devices. The individual element antenna possesses the following dimensions: A = 0.3 mm, E = 6.75 mm, M = 7 mm, N = 11 mm, DD = 1 mm, O = 4.75 mm, as depicted in Fig. 1a–b.

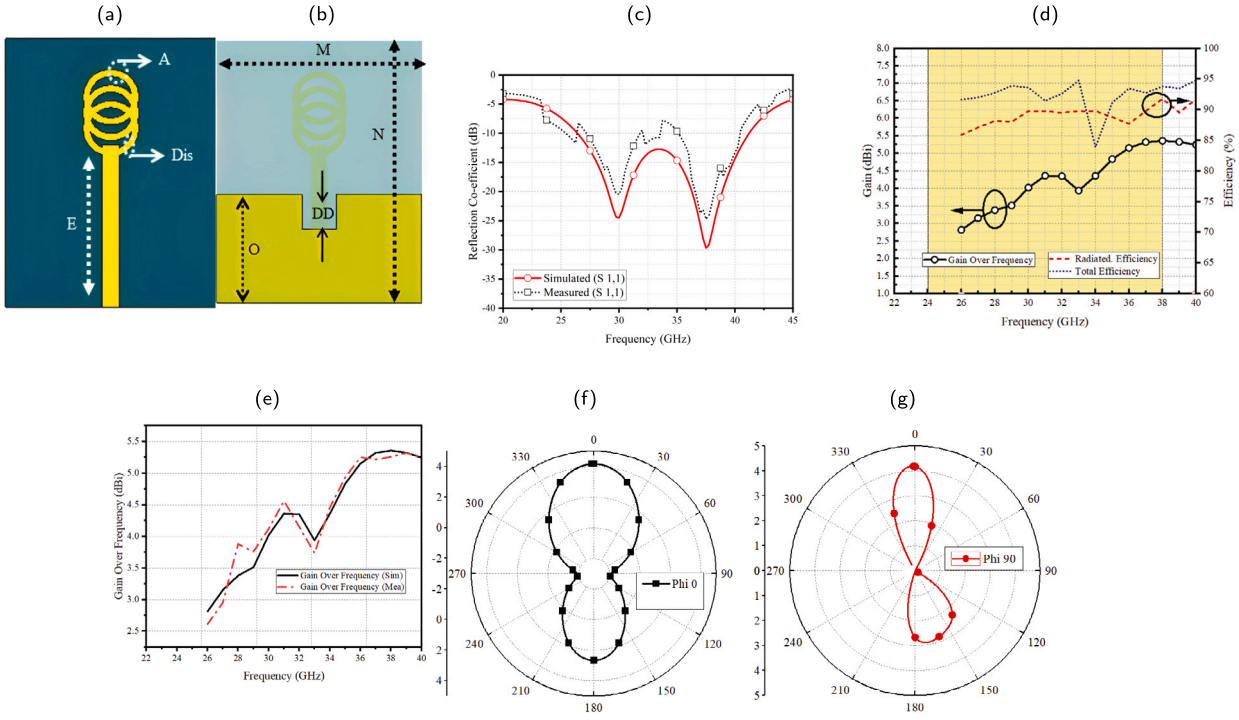

Fig. 1. Proposed Single Element Design(a) Front side; (b) Back side; (c) Simulated and Measured S(1,1); (d) Simulated Gain, Radiation and Total Efficiency; (e) Simulated and Measured Gain Over Frequency; (f) Radiation Pattern 28 GHz Φ = 0°; and (g) Radiation Pattern 28 GHz Φ = 90°.

4. Antenna design (MIMO configuration)

The proposed MIMO antenna with a tri-circular ring configuration is designed on an RO5880 substrate. The substrate has a relative permittivity of 2.3. The design and analysis of the antenna are performed using Computer Simulation Technology (CST) software, specifically version 2022. [33]. The substrate height is set to 0.254 mm, ensuring the desired characteristics and functionality of the antenna design. The proposed resonator structure includes three configurations: 1) the first circle with microstrip line, 2) Inserting the middle circle and partial ground plane, and 3) inserting the top circle and square slot on the partial ground plane. The first circle is attached to a microstrip line operating at 26-31 GHz frequency bands. The middle circle and a partial ground plane on the back side enhance the impedance bandwidth for wide-band operation, covering 26-34 GHz frequency bands. The top circle and the square slot on the partial ground plane achieve broadband characteristics spanning 26-40 GHz frequency bands. The proposed antenna layout offers two advantages: the integration of thin microstrip lines, forming a tri-circular-shaped radiator, and the use of a partial ground plane, enhanced by a small square slot, promoting wide impedance bandwidth and high isolation characteristics. The partial ground plane on the bottom side of the substrate improves isolation between antenna elements and enhances impedance matching, resulting in a broader bandwidth. The proposed partial ground plane also incorporates a thin square-shaped slot, expanding the antenna's bandwidth. The MIMO antenna has following dimensions: U = 0.3 mm, V = 6.75 mm, Y = 9 mm, X = 1 mm, W = 4.75 mm, R = 5.5 mm, S = 0.8 mm, T = 2.4 mm and U = 0.8 mm, as shown in Fig. 2a–b.

The proposed MIMO antenna elements are organized orthogonally, utilizing a polarization diversity configuration to simultaneously transmit and receive multiple independent data streams in the mmWave frequency, as depicted Fig. 2a. The proposed antenna features partial ground planes with square-shaped slots on its backside as shown in Fig. 2b, with a total size of 23×18 mm^2 while Fig. 2c shows the back view with connected ground plane. Also, the figure shows that in our design, to obtain high isolation and reduce the mutual coupling among radiating elements, there is no need to design the decoupling structures between the antenna elements. The equivalent circuit model of the proposed MIMO antenna is shown in Fig. 3. A qualitative analysis of the four antenna elements reveals that all the antenna elements are identical using the concept of parallel RLC resonator circuits Fig. 3. R_d denotes the loss that occurs due to the decoupling structure, while R_a signifies the radiation resistance. The capacitance and inductance were denoted, respectively, by the symbols L_a and C_a. Furthermore, the inductance and capacitance values associated with the complete decoupling configuration were denoted by the symbols L_d and C_d. The coupling signal can transmit electromagnetic energy to the adjacent antenna element during the operation state of the antenna. Nonetheless, it is observed that electromagnetic energy is transmitted in both directions between the two antenna elements. Hence, K_{12} and K_{21} denote the coupling energy between antenna 1 and antenna 2, whereas K_{34} and K_{43} indicate the coupling energy across element 3 and element 4.

The proposed MIMO antenna has a symmetrical structure, with equal coupling between port 1 and port 2, as well as between port 3 and port 4. Furthermore, it is noted that the coupling coefficients K_{1_2} and K_{2_1} are identical, just as K_{3_4} is equal to K_{4_3}.

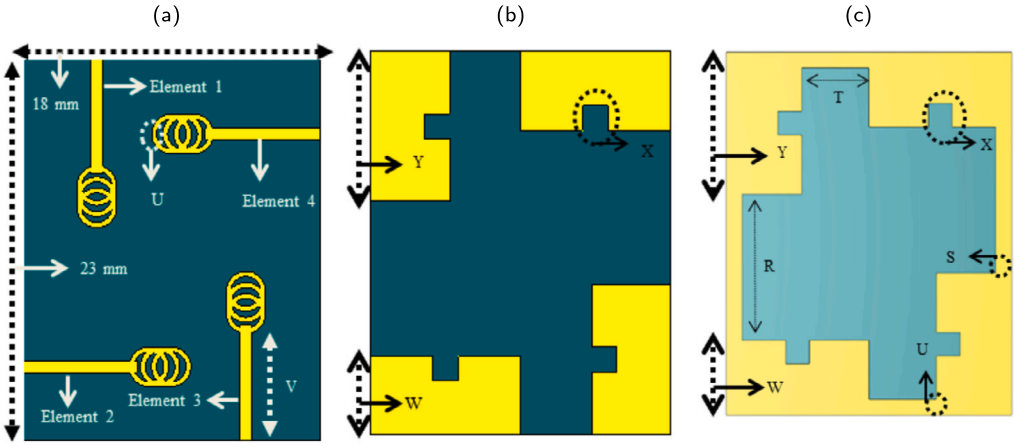

Fig. 2. Proposed MIMO antenna (a) Front side; (b) Back side Separate Ground Plane ;and (c) Back side Connected Ground Plane.

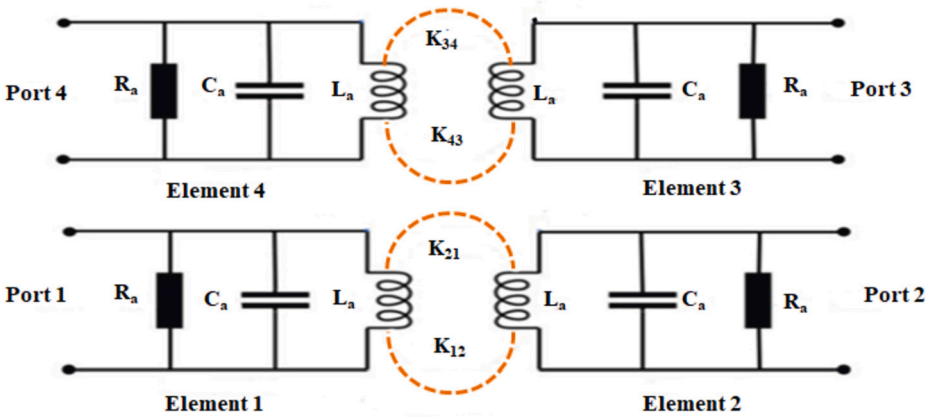

Fig. 3. MIMO antenna equivalent circuit model.

The calculation of the RLC parameters can be performed using the expression provided in [34]. Specifically, the resistance can be calculated from (1)

$$R = \frac{1}{w\sigma_{\text{cond}}\delta} \tag{1}$$

where, σ_{cond} denotes the transmission line conductivity and δ denotes the skin depth while ω represents the angular frequency which is expressed by

$$\delta = \frac{1}{\sqrt{\pi f \mu_0 \sigma_{\text{cond}}}}$$

The internal inductance per unit length can be expressed as (2)

$$L = \frac{1}{w\sigma_{\text{cond}}\omega\delta} \tag{2}$$

where w denotes the width of the transmission line and the capacitance is calculated from (3)

$$C = \frac{\varepsilon w}{d} \tag{3}$$

where, ε represents the permittivity of the dielectric medium and finally, per unit length conductance is expressed as (4)

$$G = \frac{\sigma_{\text{dielec}} w}{d} \tag{4}$$

The S-Parameters of the proposed antenna show a wide-band response from 26 to 40 GHz, as shown in Fig. 4 with suitable performance characteristics. Fig. 4a shows the simulated S-parameters of the four elements, which shows the frequency response of S (1,1), S (2,2), S(3,3) and S(4,4). In the S(1,1) and S(2,2) curves, the peak reflection coefficient of 30 dB is observed at 38 GHz, while 23.5 dB is noted at 28 GHz, which covers the frequency range of 26-40 GHz. Furthermore, in S(3,3) and S(4,4) curves, the peak reflection coefficient of 33.46 dB is noted at 38 GHz, while 22.23 dB is observed at 28 GHz with an impedance bandwidth of 14

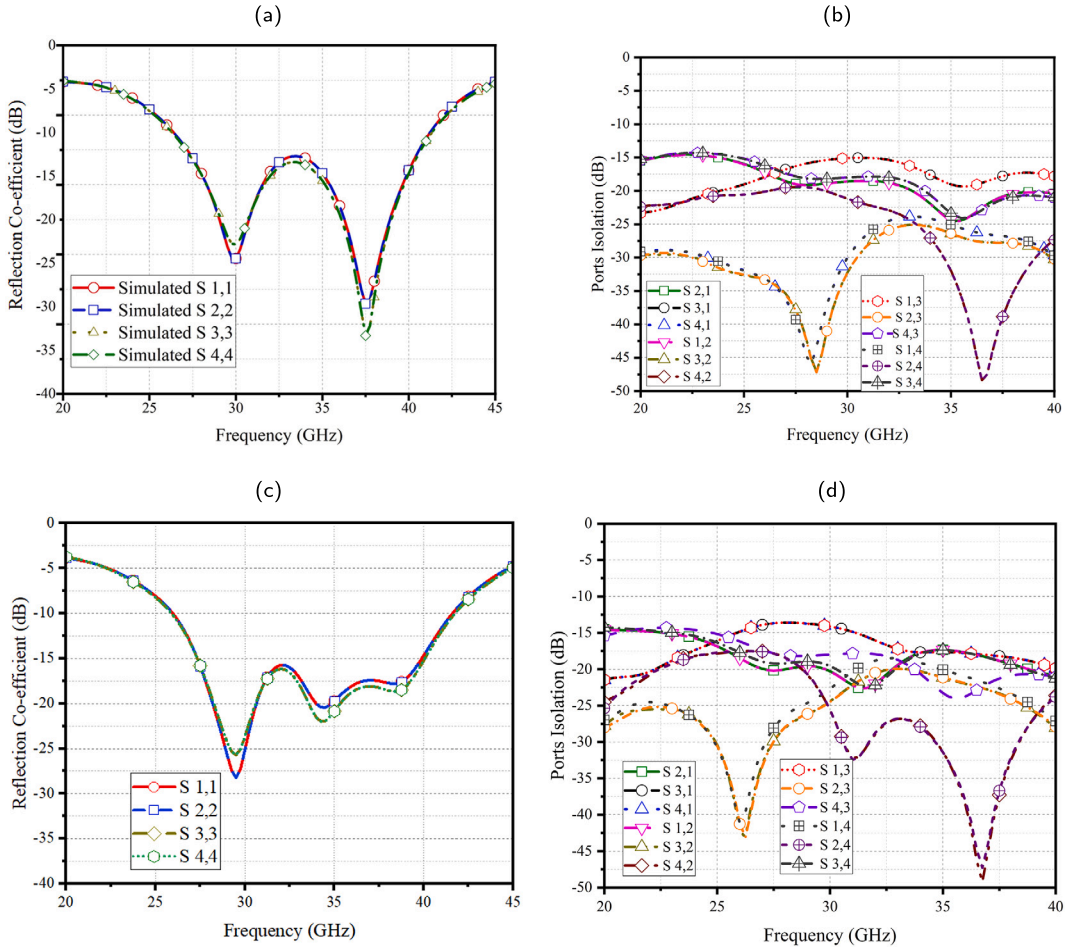

Fig. 4. Simulated MIMO S-parameters (a) Reflection Co-efficient with Separated Ground Plane ; (b) Ports isolation with Separated Ground Plane; (c) Reflection Co-efficient with Connected Ground Plane; and (d) Ports isolation with Connected Ground Plane.

GHz. The simulated results of port isolation are shown in Fig. 4b. The isolation is found to be great at -18 dB at the 28 GHz frequency band, while -19 dB is noted at the 38 GHz band, confirming the effective isolation between the antenna elements. Fig. 4c shows the S-parameters of the four elements with connected ground plane while Fgure 4d shows the simulated results of ports isolation with connected ground plane. According to the simulation results, the designed MIMO antenna shows acceptable resonance behavior throughout the specified frequency bands. It offers sufficient isolation between the antenna elements, ensuring reliable and effective communication performance.

5. Prototype development and measurement

Leiterplatten-Kopierfrasen (LPKF) machine was used for the fabrication of the proposed tri-circular MIMO antenna [27] and [35]. The testing and validation were performed using in-house facilities of Pakistan Aeronautical Complex (PAC), Kamra, Pakistan. The fabricated prototype is shown in Fig. 5. Fig. 5a shows the front view of the MIMO antenna without connectors, and Fig. 5b shows the back view of the antenna without connectors while Fig. 5c shows the front view with Sub-Miniature Push-on Micro (SMPM) male connectors. A scale and coin have been placed close to the fabricated prototype in order to confirm its physical length.

The simulated and measured MIMO antenna S-parameters of the four antenna elements are shown in Fig. 6a–d. The solid-red curves show the simulated results, whereas the dotted-black curves show the measured results. The measured results show some ripple disruptions from the simulated results, but overall, the results are well agreed upon for a good MIMO system. The reflection coefficient of the measured results shows that the MIMO system is operating at 28 and 38 GHz, and the return loss is less than -10 dB over the desired band (i.e., 26-40 GHz).

Slight disruptions are also observed from measured results of port isolation, but these results matched the simulated results achieved from simulations. The port isolation measured results are shown in Fig. 7. In Fig. 7a, it can be clearly seen that the measured isolation value is obtained from S(2,1) as -19 dB at 28 GHz and -19.5 dB at 38 GHz. Fig. 7b shows the measured port isolation obtained from S(3,1) where -17 dB is achieved at 28 GHz and -18 dB at 38 GHz.

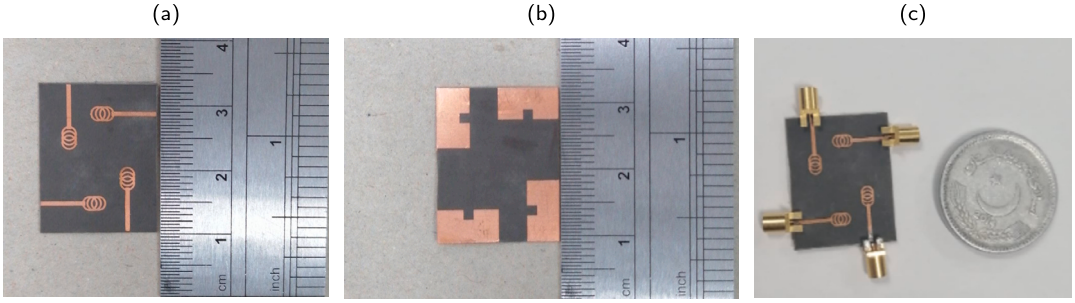

Fig. 5. Prototype of the proposed antenna: (a) Front view without connectors (b) Back view without connectors (c) Front view with connectors.

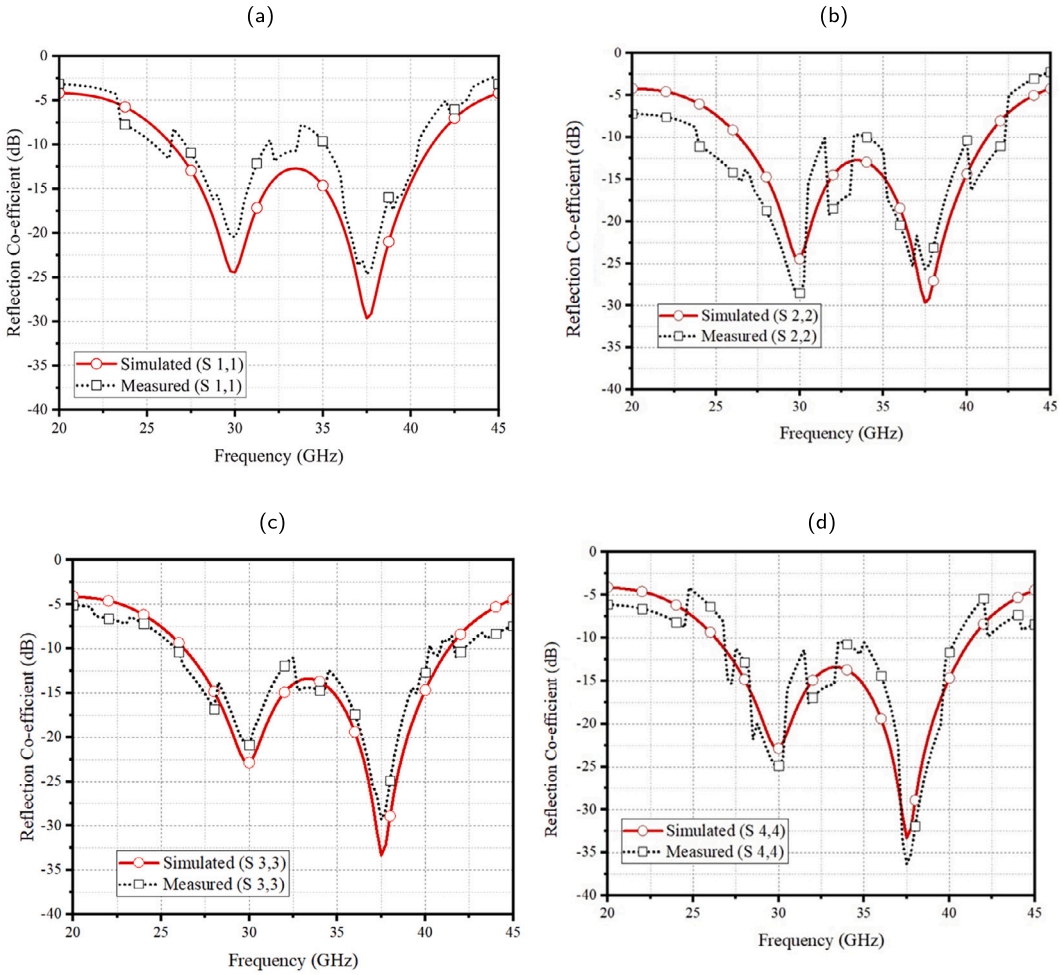

Fig. 6. Measured S-parameters of the MIMO antenna (a) S(1,1) (b) S(2,2) (c) S(3,3), and (d) S(4,4).

The simulated (Sim) and measured (Mea) radiation patterns of two planes, Phi (90°) and Theta (90°), for two arbitrary antenna elements, element 1 and element 2, are shown in Fig. 8. Where (Sim) shows the simulated results while (Mea) presents the measured results. In Fig. 8a, we indicate the radiation pattern for element 1 at 28 GHz and Phi (90°). The results indicate that the main lobe direction is at 169°. For element 2 and using the same frequency, Fig. 8b shows that the main lobe is at 35°. Fig. 8c and Fig. 8d display the radiation pattern for elements 1 and 2 at 38 GHz frequency and Theta (90°). The main lobe direction is at 51° for element 1 while for element 2 is at 318°. Again, there are slight disruptions in the measured results, but the results are successfully matched with the simulations.

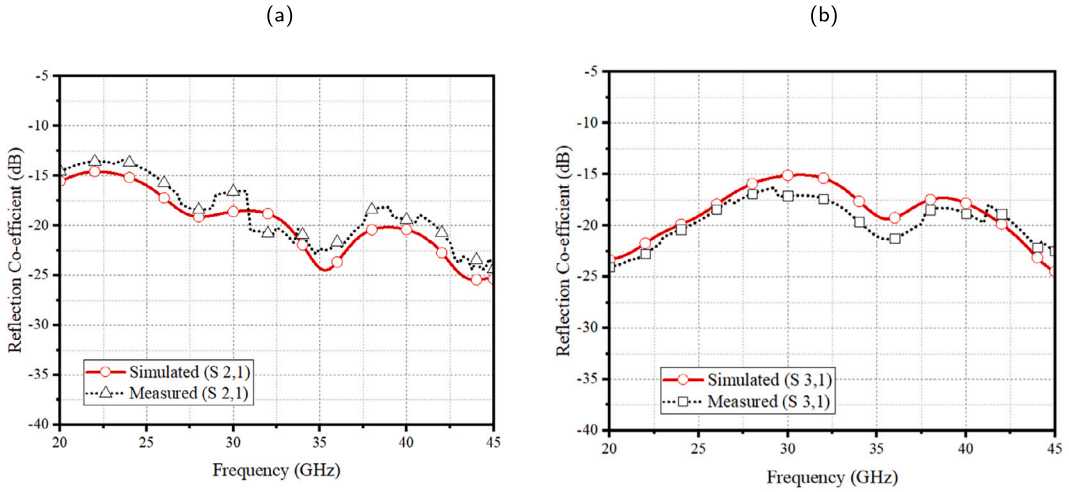

Fig. 7. Measured ports isolation of MIMO antenna (a) S(2,1); (b) S(3,1).

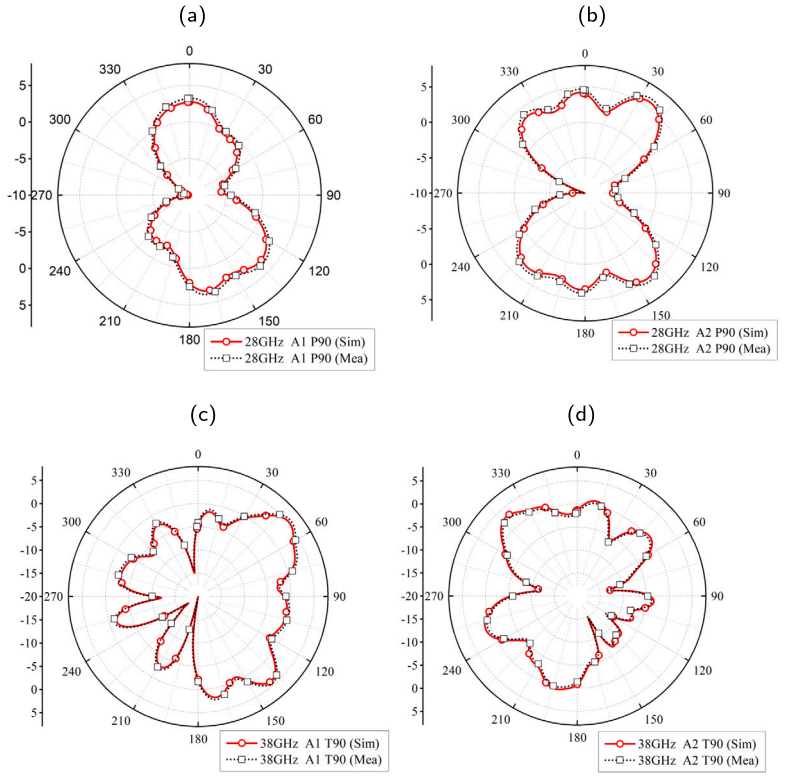

Fig. 8. MIMO antenna simulated and measured radiation pattern (a) Element 1 at 28 GHz and Phi (90°); (b) Element 2 at 28 GHz and Phi (90°); (c) Element 1 at 38 GHz and Theta (90°); (d) Element 2 at 38 GHz and Theta (90°).

The 3D gain of the proposed MIMO antenna at 28 GHz is shown in Fig. 9a–d for the four elements. The obtained gain for the elements 1, 2, 3, and 4 are 4.7 dBi, 6.09 dBi, 4.66 dBi, and 6.6 dBi, respectively. Each antenna element gain is satisfactory for the frequency band of 28 GHz.

Antenna gain is an important parameter in antenna design, which refers to the antenna's ability to focus the radiation in a particular direction compared to an isotropic radiator. A higher gain value indicates that the antenna is more effective at concentrating energy in the desired direction, resulting in increased coverage, improved signal strength, and better communication range. Fig. 10a shows the simulated and measured gain of the proposed antenna. The measured gain varies between 4 dBi to 6.1 dBi. At 28 GHz, the gain of the antenna is observed as 4.5 dBi, while at 38 GHz, the antenna gain is noted as 6.1 dBi, which is suitable for smart 5G devices.

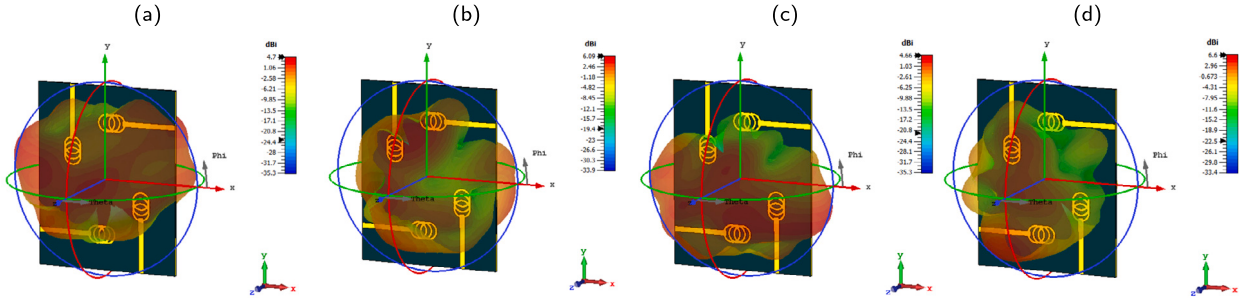

Fig. 9. The gain of the proposed antenna in 3D at 28 GHz: (a) Element 1, (b) Element 2, (c) Element 3, and (d) Element 4.

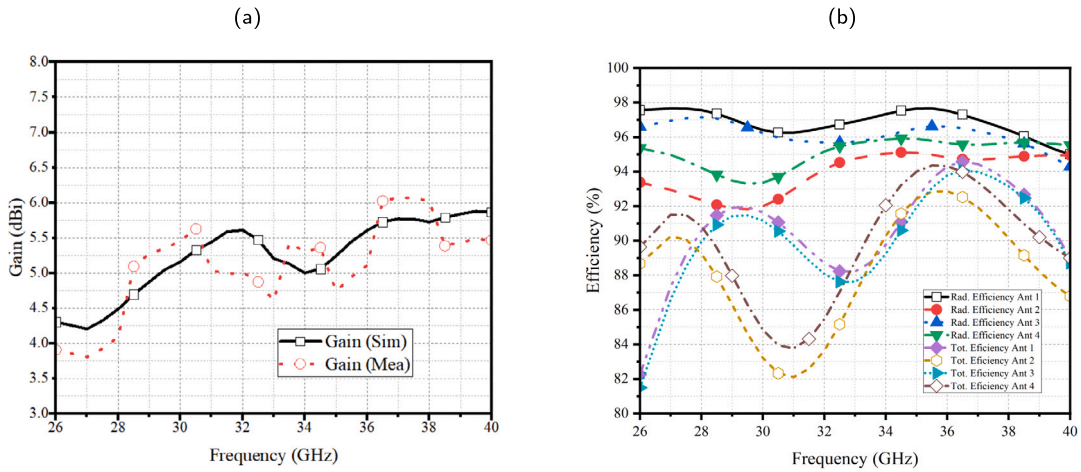

Fig. 10. (a) Simulated and measured gain, and (b) Radiation and total efficiency.

Radiation efficiency measures the effectiveness of an antenna in converting input power into radiated electromagnetic waves. A higher radiated efficiency indicates that a larger portion of the input power is effectively radiated, resulting in better overall antenna performance. Furthermore, total efficiency represents the ratio of the total power radiated by the antenna to the total input power supplied to the antenna, considering the radiated power and the mismatch loss throughout the antenna system. The total efficiency is calculated from (5) as follows [36]

$$\eta_{\text{total}} = \eta_{\text{radiation}} \times \eta_{\text{conduction}} \times \eta_{\text{dielectric}} \times \eta_{\text{mismatch}} \tag{5}$$

where,

- $\eta_{\text{radiation}}$ is the radiation efficiency, which accounts for how efficiently the antenna radiates energy into space.
- $\eta_{\text{conduction}}$ is the conduction efficiency, which takes into account the losses in the conductive elements of the antenna, such as metallic components.
- $\eta_{\text{dielectric}}$ is the dielectric efficiency, which considers losses in the dielectric materials, such as insulators or substrates used in antenna construction.
- η_{mismatch} is the mismatch efficiency, which quantifies the losses that occur when there is a mismatch between the antenna and the transmission line or an impedance mismatch within the antenna.

It's worth observing that achieving high efficiency in mmWave antennas is a challenging task due to various factors, including the compact size of the antenna elements, high operating frequencies, and the potential for increased losses at these frequencies. Design considerations such as antenna geometry, substrate materials, feeding techniques, and impedance matching can influence the efficiency of an mmWave antenna. The radiation and total efficiency of the proposed antenna are presented in Fig. 10b, where the (Sim) shows the simulated results and (Mea) presents the measured results. The results show that the minimum radiation and total efficiency are achieved on element 2, which is observed as 92% at 28 GHz and 95% at 38 GHz, while the total efficiency is noted as 89% at 28 GHz and 90% at 38 GHz, respectively.

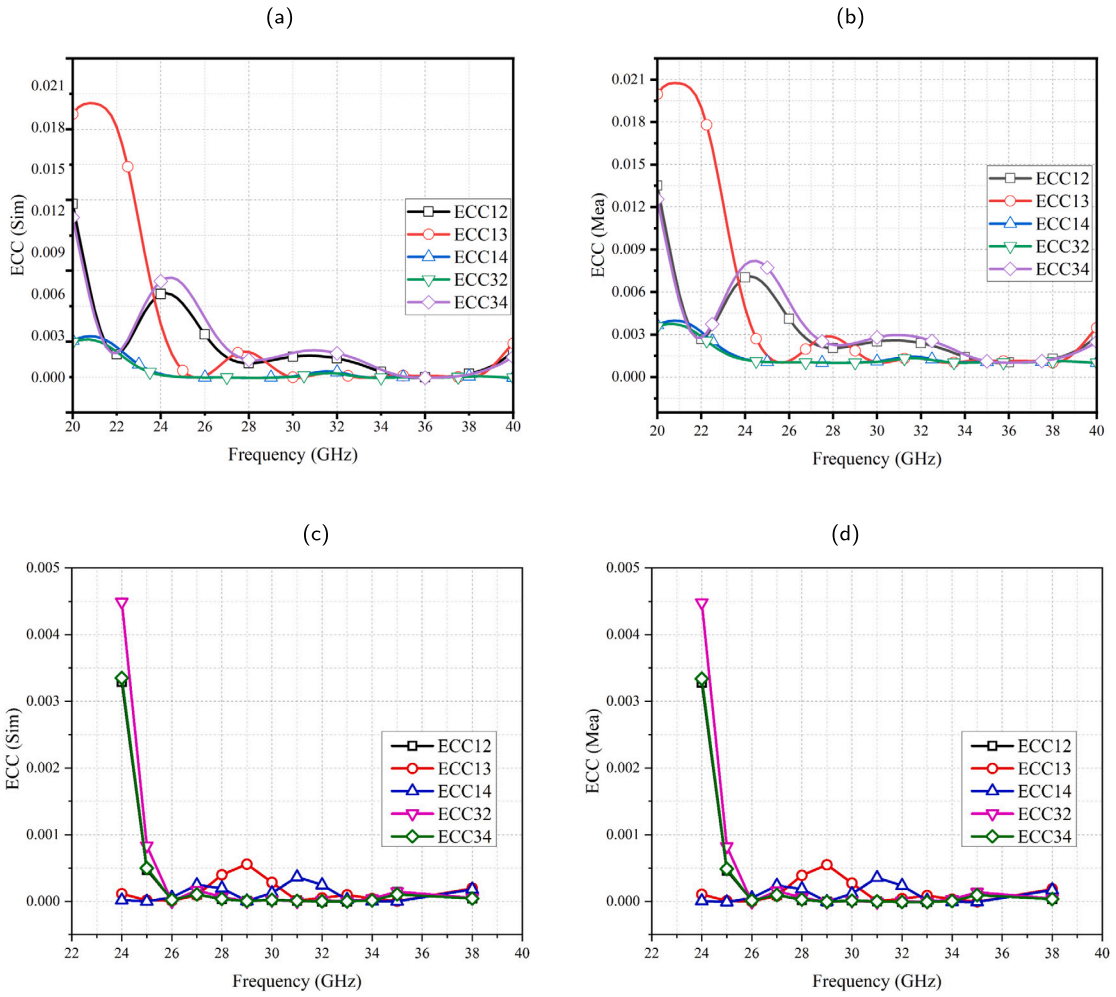

Fig. 11. MIMO antenna ECC parameter results (a) ECC (Sim); (b) ECC (Mea); (c) ECC (Sim) from Radiation Pattern; and (d) ECC (Mea) from radiation Pattern.

6. MIMO performance parameters

The most important parameters of the MIMO system are the ECC, DG, Mean Effective Gain (MEG), Total Active Reflection Coefficient (TARC), and Channel Capacity Loss (CCL). ECC is defined as the impact of one antenna on the performance of another antenna in a MIMO system. In practical scenarios, ECC values are preferred to remain below 0.5 [37]. It can be derived using (6) and is given mathematically by [37]

$$ECC = \frac{\left| \iint_{4\pi} \left(\vec{\beta}_i(\theta,\emptyset)\right) \times \left(\vec{\beta}_j(\theta,\emptyset)\right) d\Omega \right|^2}{\iint_{4\pi} \left| \left(\vec{\beta}_i(\theta,\emptyset)\right) \right|^2 d\Omega \iint_{4\pi} \left| \left(\vec{\beta}_j(\theta,\emptyset)\right) \right|^2 d\Omega} \tag{6}$$

where, $\left(\vec{\beta}_i(\theta,\emptyset)\right)$ and $\left(\vec{\beta}_j(\theta,\emptyset)\right)$ represents the 3D radiation pattern established when the ith and jth antenna elements are excited, respectively, while Ω denotes the solid angle. ECC simulated results are compared with measured results as shown in Fig. 11. Fig. 11a shows the simulated results while the measured results are shown in Fig. 11b. In both figures, it can be seen that the simulated and the measured ECC results are less than 0.5. The ECC values at 28 GHz and 38 GHz are 0.0017 and 0.0016, respectively, which show that the antenna elements are well isolated within the frequency range of 26-40 GHz and can be used for practical 5G devices. The highest ECC of 0.020 and 0.018 were observed outside the frequency range at 22 and 23 GHz, respectively, which shows that the antenna elements are not properly isolated at these frequency bands. ECC is also calculated with the help of radiation pattern for the frequency band of 24-38 GHz, as shown in Fig. 11c and Fig. 11d.

Spatial diversity uses the multipath channel to prevent multipath fading by sending different sorts of the same transmitted signals to the receiver. The receiver can use one of the diversity coupling methods to improve the wireless network's reliability. This improvement is calculated using the DG metric. The DG is calculated from (7) as follows [36]

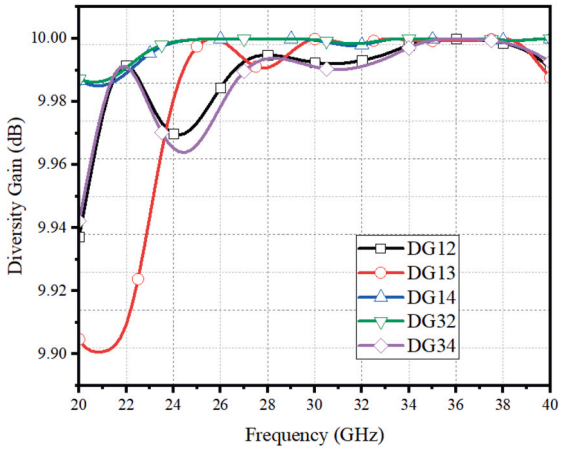

Fig. 12. DG parameters results of the designed antenna.

Table 1
Proposed MIMO Antenna MEG.

Frequency (GHz)	MEG 1 (dB)	MEG 2 (dB)	MEG 3 (dB)	MEG 4 (dB)
28 GHz	-3.16	-3.21	-3.19	-3.73
38 GHz	-2.98	-3.62	-3.51	-3.31

$$DG\ (dB) = 10 \times \sqrt{1 - (ECC)^2} \tag{7}$$

The standard range for DG in MIMO systems typically lies between 9.95 to 10 dB and can be used for practical 5G devices. The DG results are presented in Fig. 12, where it can be observed that at 28 GHz, the DG is noted as 9.98 dB while at 38 GHz, it is observed as 9.9 dB, which shows that the results are within the acceptable limits. The ability of an antenna to receive microwave energy in a multipath environment is evaluated by MEG. MEG is defined as the proportion of the antenna's mean received power to its mean incident power [38]. It can be obtained from (8) and expressed mathematically by

$$MEG = \int_{-\pi}^{\pi} \int_{0}^{\pi} \left[\frac{r}{r+1} G_\theta(\theta,\phi) P_\theta(\theta,\phi) + \frac{1}{1+r} G_\phi(\theta,\phi) P_\phi(\theta,\phi) \right] sin\theta d\theta d\phi \tag{8}$$

where, $G_\phi(\theta,\phi)$ and $P_\theta\,(\theta,\ \phi)$ represents the angle of arrival and r denotes the cross-polar ratio which can be mathematically stated as

$$r = 10log_{10}\left(\frac{P_{vpa}}{P_{hpa}}\right)$$

where, P_{vpa} and P_{hpa} represent the power with vertical and horizontal polarization antenna.

It can be noted that at 28 GHz, the MEG of element 1 is observed as -3.16 dB, element 2 is -3.21 dB, element 3 is -3.19 dB, and element 4 is -3.73 dB, while at 38 GHz, the MEG of element 1 is noted as -2.98 dB, element 2 is -3.62 dB, element 3 is -3.51 dB, and element 4 is -3.31. These values are well below the practical value threshold of 1 dB at the desired frequency bands. Table 1 shows the MEG of the proposed MIMO system of each antenna element, i.e., elements 1, 2, 3, and 4 at 28 GHz and 38 GHz.

The CCL is a significant performance parameter that defines the maximum achievable transmission rate while maintaining a loss of less than 0.4 bits/s/Hz. It is a crucial metric for assessing diversity performance in practical MIMO systems. [39]. The CCL is calculated from (9)

$$C_{loss} = -log_2 \det\left(\alpha^R\right) \tag{9}$$

where, $\left(\alpha^R\right)\}$ represents the correlation matrix defined by

$$\alpha^R = \begin{bmatrix} \alpha_{11} & \cdots & \alpha_{14} \\ \vdots & \ddots & \vdots \\ \alpha_{41} & \cdots & \alpha_{44} \end{bmatrix}$$

where $\alpha_{ij} = S_{ii}^* S_{ij} + S_{ji}^* S_{ij}$ and S_{i_j} denotes the measured S-parameters. The simulated and measured results of the performance of the proposed antenna in term of the CCL parameter are shown in Fig. 13a. It can be noted that the simulation and the measured results of the CCL parameter are less than the threshold value of 0.4 bits/s/Hz in the operating frequency band, i.e., 26-40 GHz. Moreover,

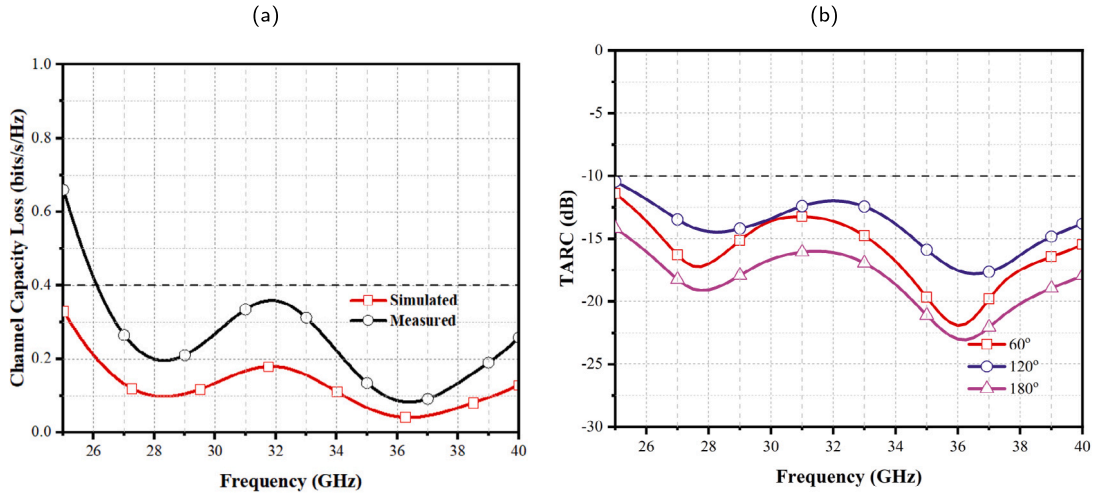

Fig. 13. (a) Performance of the MIMO antenna in terms of CCL, (b) MIMO antenna parameters TARC.

Table 2
Comparison with other published work.

Ref	O.F (GHz)	B.W (GHz)	Size (mm^2)	Size (λ)	Ground Plane	Gain (dBi)	Isolation (dB)	Eff. (%)	ECC	Comm.
[12]	27.6-28.6/ 37.4-38.6	1/ 1.2	20×24	0.18×0.23	C	7.9	28	>85	0.001	mmWave 5G
[13]	23-40	17	80×80	0.84× 0.84	C	12	>20	>70	0.0014	5G devices
[14]	1.8-2.6/ 25-40	0.8/ 15	25×12	0.18×0.08	C	7.2	>17	65	0.01	4G and 5G devices
[18]	27-30	3	30×30	0.28×0.28	NC	6.1	<29	92	0.016	mmWave devices
[26]	26-30	4	31×31	0.27×0.27	NC	3.2	<22	80	<0.015	mmWave devices
[27]	22.4-31.6	9.23	30×30	0.21×0.21	NC	5.6	>25	>80	0.16	mmWave devices
[30]	7.55-22.8	15.3	138×69	6.9×3.45	C	6.9	>18	85	0.061	Vehicular devices
[31]	1.95-6.25	4.3	50×50	0.64×0.64	C	3.3	16.5	88.5	0.028	5G devices
[33]	27.5-30.9/ 37.3-44.6	3.4 7.3	40.4×20	3.77×1.86	C	5.7 9.5	20 18	85 88.2	0.001	5G devices
Prop.	26-40	14	23×18	0.26× 0.20	NC	6.6	>18	>90	0.001	mmWave 5G portable devices

O.F = Operating Frequency, B.W = Bandwidth, Eff. = Efficiency, C = Connected, NC = Not Connected Comm. = Communication.

at 28 GHz the simulated CCL is noted as 0.1 bits/s/Hz while at 38 GHz it is indicated as 0.16 bits/s/Hz, which satisfies the acceptable limit condition of a MIMO system.

The TARC is a metric used to assess a MIMO system's power efficiency and performance. It measures the ratio between the total power reflected by the antennas and the actual power incident on the antennas. A low TARC value indicates the efficient transmission of signals in a MIMO system with minimal losses caused by reflection, which leads to better signal quality, faster data rates, and improved capacity in the system for outstanding communication. It is expressed using (10) and calculated for a four-port MIMO antenna by [39]

$$TARC = \frac{\sqrt{\begin{array}{l}\left|S_{11}+S_{12}e^{j\theta_1}+S_{13}e^{j\theta_2}+S_{14}e^{j\theta_3}\right|^2 \\ +\left|S_{21}+S_{22}e^{j\theta_1}+S_{23}e^{j\theta_2}+S_{24}e^{j\theta_3}\right|^2 \\ +\left|S_{31}+S_{32}e^{j\theta_1}+S_{33}e^{j\theta_2}+S_{34}e^{j\theta_3}\right|^2 \\ +\left|S_{41}+S_{42}e^{j\theta_1}+S_{43}e^{j\theta_2}+S_{44}e^{j\theta_3}\right|^2\end{array}}}{\sqrt{N}} \tag{10}$$

where θ denotes the phase angle of the MIMO system, and N represents the number of antenna elements. It is clear from Fig. 13b that the TARC is less than -10 dB in all the frequencies of the desired band. Moreover, in Fig. 13b the impact of θ is studied, where θ is increased from 60° to 180° with a step size of 60°. It is observed that as θ increases, the TARC value drops below -10 dB, which shows the signals are efficiently transmitted from a MIMO system.

Finally, the proposed antenna is compared with previously published literature as shown in Table 2. It is noted that the proposed MIMO system delivers good gain with a minimum antenna size of 23×18 mm^2 and wideband characteristics. All the investigated performance parameters have been determined to fall within acceptable limits and satisfy the performance requirements for the proposed MIMO system, which is appropriate for both realistic 5G and mmWave applications.

7. Conclusions

This design presents a MIMO tri-circular shape mmWave antenna with orthogonal MIMO assembly on a thin RO5880 with a permittivity of 2.3, and substrate height is kept at 0.254 mm. The antenna showed a wide frequency range of 26 to 40 GHz, with gain varying between 4 and 6.6 dBi. At 28 GHz, it was noted to be 6.6 dBi with radiation efficiency greater than 90%. In addition, it is noted that improved isolation is found among radiating elements, which indicates minimal coupling or interference between the radiating elements and enables better independent transmission and reception of signals, leading to improved performance. The dimension of the MIMO antenna is 23×18 mm^2 with an impedance bandwidth of 14 GHz, which is smaller than compared to previously published techniques and covers the 5G frequency bands of 26, 28, 32 and 38 GHz. In addition, for the proposed MIMO design, the performance parameters MEG, ECC, DG, CCL, and TARC are also calculated. The simulated and evaluated results are compared with the stated literature and are found to be in acceptable agreement. The proposed antenna system is found to be an appropriate candidate for practical future 5G and mmWave applications.

CRediT authorship contribution statement

Mehr E. Munir: Writing – original draft, Software, Methodology, Investigation, Data curation, Conceptualization. **Moustafa M. Nasralla:** Validation, Supervision, Investigation. **Maged Abdullah Esmail:** Writing – review & editing, Visualization, Resources, Project administration, Funding acquisition, Data curation.

Declaration of competing interest

The authors declare the following financial interests/personal relationships which may be considered as potential competing interests:

DR. Mehr E Munir reports financial support was provided by Prince Sultan University. Dr. Mehr E Munir reports a relationship with Prince Sultan University that includes: employment. If there are other authors, they declare that they have no known competing financial interests or personal relationships that could have appeared to influence the work reported in this paper.

Data availability

All the data is available in this study.

Acknowledgements

The authors would like to acknowledge Prince Sultan University and Smart Systems Engineering lab for their valuable support. Also, the authors would like to acknowledge the support of Prince Sultan University for paying the Article Processing Charges (APC) of this publication. The authors would also like to acknowledge the team of RF Engineering group, Aircraft Rebuild Factory, Pakistan Aeronautical Complex, Kamra, Pakistan for its valuable support in testing and validation.

This work was supported by the research grants [SEED-2023-CE-143]; Prince Sultan University; Saudi Arabia [grant number SEED-2023-CE-143.]

References

[1] Thennarasi Govindan, Sandeep Kumar Palaniswamy, Malathi Kanagasabai, Sachin Kumar, Mohamed Marey, Hala Mostafa, Design and analysis of a flexible smart apparel MIMO antenna for bio-healthcare applications, Micromachines 13 (11) (2022) 1919.

[2] Saad Hassan Kiani, Mohamed Marey, Hüseyin Şerif Savci, Hala Mostafa, Umair Rafique, Muhammad Amir Khan, Dual-band multiple-element MIMO antenna system for next-generation smartphones, Appl. Sci. 12 (19) (2022) 9694.

[3] Saad Hassan Kiani, Muhammad Abbas Khan, Umair Rafique, Mohamed Marey, Abdullah G. Alharbi, Hala Mostafa, Muhammad Amir Khan, Syed Muzahir Abbas, High performance eight-port dual-band MIMO antenna system for 5G devices, Micromachines 13 (6) (2022) 959.

[4] Diego Fernando Carrera, Cesar Vargas-Rosales, David Zabala-Blanco, Noe M. Yungaicela-Naula, Cesar A. Azurdia-Meza, Mohamed Marey, Ali Dehghan Firooz-abadi, Novel multilayer extreme learning machine as a massive MIMO receiver for millimeter wave communications, IEEE Access 10 (2022) 58965–58981.

[5] Mehr E. Munir, Saad Hassan Kiani, Huseyin Serif Savci, Daniyal Ali Sehrai, Fazal Muhammad, Ayyaz Ali, Hala Mostafa, Naser Ojaroudi Parchin, mmwave polarization diversity wideband multiple-input/multiple-output antenna system with symmetrical geometry for future compact devices, Symmetry 15 (9) (2023) 1641.

[6] Walid Dyab, Ahmed A. Sakr, Ke Wu, Millimeter-wave polarization-inclusive remote sensing system based on dually-polarized six-port junction, in: 2018 11th Global Symposium on Millimeter Waves (GSMM), IEEE, 2018, pp. 1–3.

[7] Ahmed A. Sakr, Walid Dyab, Ke Wu, Image theory based miniaturization of nonradiative dielectric coupler for millimeter wave integrated circuits, in: 2017 IEEE MTT-S International Microwave Symposium (IMS), IEEE, 2017, pp. 463–465.

[8] Mourad S. Ibrahim, Low-cost, circularly polarized, and wideband U-slot microstrip patch antenna with parasitic elements for WiGig and WPAN applications, in: 2019 13th European Conference on Antennas and Propagation (EuCAP), IEEE, 2019, pp. 1–4.

[9] Vincent W.S. Wong, Robert Schober, Derrick Wing Kwan Ng, Li-Chun Wang, Key Technologies for 5G Wireless Systems, Cambridge University Press, 2017.

[10] Fei Hu, Opportunities in 5G Networks: A Research and Development Perspective, CRC Press, 2016.

[11] Qian Zhu, Kung Bo Ng, Chi Hou Chan, Kwai-Man Luk, Substrate-integrated-waveguide-fed array antenna covering 57–71 GHz band for 5G applications, IEEE Trans. Antennas Propag. 65 (12) (2017) 6298–6306.

[12] Kiran Raheel, Ahsan Altaf, Arbab Waheed, Saad Hassan Kiani, Daniyal Ali Sehrai, Faisel Tubbal, Raad Raad, E-shaped H-slotted dual band mmwave antenna for 5G technology, Electronics 10 (9) (2021) 1019.

[13] Daniyal Ali Sehrai, Mujeeb Abdullah, Ahsan Altaf, Saad Hassan Kiani, Fazal Muhammad, Muhammad Tufail, Muhammad Irfan, Adam Glowacz, Saifur Rahman, A novel high gain wideband MIMO antenna for 5G millimeter wave applications, Electronics 9 (6) (2020) 1031.
[14] Emad Al Abbas, Muhammad Ikram, Ahmed Toaha Mobashsher, Amin Abbosh, MIMO antenna system for multi-band millimeter-wave 5G and wideband 4G mobile communications, IEEE Access 7 (2019) 181916–181923.
[15] Muhammad Asif, Daniyal Ali Sehrai, Saad Hassan Kiani, Jalal Khan, Mujeeb Abdullah, Muhammad Ibrar, Mohammad Alibakhshikenari, Francisco Falcone, Ernesto Limiti, Design of a dual band SNG metamaterial based antenna for LTE 46/WLAN and Ka-band applications, IEEE Access 9 (2021) 71553–71562.
[16] Seong-Jin Park, Dong-Hun Shin, Seong-Ook Park, Low side-lobe substrate-integrated-waveguide antenna array using broadband unequal feeding network for millimeter-wave handset device, IEEE Trans. Antennas Propag. 64 (3) (2015) 923–932.
[17] Hidayat Ullah, Farooq A. Tahir, A broadband wire hexagon antenna array for future 5G communications in 28 GHz band, Microw. Opt. Technol. Lett. 61 (3) (2019) 696–701.
[18] Mian Muhammad Kamal, Shouyi Yang, Xin-cheng Ren, Ahsan Altaf, Saad Hassan Kiani, Muhammad Rizwan Anjum, Amjad Iqbal, Muhammad Asif, Sohail Imran Saeed, Infinity shell shaped MIMO antenna array for mm-wave 5G applications, Electronics 10 (2) (2021) 165.
[19] Yong-Ling Ban, Chuan Li, Gang Wu, Kin-Lu Wong, et al., 4G/5G multiple antennas for future multi-mode smartphone applications, IEEE Access 4 (2016) 2981–2988.
[20] Yixin Li, Yong Luo, Guangli Yang, et al., 12-port 5G massive MIMO antenna array in sub-6GHz mobile handset for LTE bands 42/43/46 applications, IEEE Access 6 (2017) 344–354.
[21] Jian-Feng Li, Duo-Long Wu, Bei Huang, Yan-Jie Wu, A LTE smartphone antenna with an internal matching circuit to cover 698–2710 MHz, Microw. Opt. Technol. Lett. 59 (9) (2017) 2405–2411.
[22] Joni Kurvinen, Henri Kähkönen, Anu Lehtovuori, Juha Ala-Laurinaho, Ville Viikari, Co-designed mm-wave and LTE handset antennas, IEEE Trans. Antennas Propag. 67 (3) (2018) 1545–1553.
[23] Yu-Xiang Sun, Kwok Wa Leung, Substrate-integrated two-port dual-frequency antenna, IEEE Trans. Antennas Propag. 64 (8) (2016) 3692–3697.
[24] Mohammad S. Sharawi, Symon K. Podilchak, Mohamed T. Hussain, Yahia M.M. Antar, Dielectric resonator based MIMO antenna system enabling millimetre-wave mobile devices, IET Microw. Antennas Propag. 11 (2) (2017) 287–293.
[25] Ayman Ayd R. Saad, Hesham A. Mohamed, Printed millimeter-wave MIMO-based slot antenna arrays for 5G networks, AEÜ, Int. J. Electron. Commun. 99 (2019) 59–69.
[26] Saifur Rahman, Xin-cheng Ren, Ahsan Altaf, Muhammad Irfan, Mujeeb Abdullah, Fazal Muhammad, Muhammad Rizwan Anjum, Salim Nasar Faraj Mursal, Fahad Salem AlKahtani, Nature inspired MIMO antenna system for future mmwave technologies, Micromachines 11 (12) (2020) 1083.
[27] Muhammad Abbas Khan, Abdullah G. Al Harbi, Saad Hassan Kiani, Anis Nurashikin Nordin, Mehr E. Munir, Sohail Imran Saeed, Javed Iqbal, Esraa Mousa Ali, Mohammad Alibakhshikenari, Mariana Dalarsson, mmwave four-element MIMO antenna for future 5G systems, Appl. Sci. 12 (9) (2022) 4280.
[28] Mahnoor Khalid, Syeda Iffat Naqvi, Niamat Hussain, MuhibUr Rahman, Seyed Sajad Mirjavadi, Muhammad Jamil Khan, Yasar Amin, et al., 4-port MIMO antenna with defected ground structure for 5G millimeter wave applications, Electronics 9 (1) (2020) 71.
[29] Wensong Wang, Zhongyuan Fang, Kai Tang, Xixi Wang, Zhou Shu, Zhenyu Zhao, Yuanjin Zheng, Wideband gain enhancement of MIMO antenna and its application in FMCW radar sensor integrated with CMOS-based transceiver chip for human respiratory monitoring, IEEE Trans. Antennas Propag. 71 (1) (2022) 318–329.
[30] Wensong Wang, Yuanjin Zheng, Wideband gain enhancement of a dual-polarized MIMO vehicular antenna, IEEE Trans. Veh. Technol. 70 (8) (2021) 7897–7907.
[31] Vishakha Thakur, Naveen Jaglan, Samir Dev Gupta, Side edge printed eight-element compact MIMO antenna array for 5G smartphone applications, J. Electromagn. Waves Appl. 36 (12) (2022) 1685–1701.
[32] Yi-Fan Tsao, Arpan Desai, Heng-Tung Hsu, Dual-band and dual-polarization CPW fed MIMO antenna for fifth-generation mobile communications technology at 28 and 38 GHz, IEEE Access 10 (2022) 46853–46863.
[33] Cst microwave studio, Computer Simulation Technology (CST), 2022.
[34] Baskaran Kasi, Yanti Erana Jalil, Chandan Kumar Chakrabarty, Circuit modeling for UWB-MIMO antenna array, in: 2013 IEEE International RF and Microwave Conference (RFM), IEEE, 2013, pp. 66–70.
[35] Ayyaz Ali, Mehr E. Munir, Moustafa M. Nasralla, Maged A. Esmail, Ahmed Jamal Abdullah Al-Gburi, Farooq Ahmed Bhatti, Design process of a compact tri-band MIMO antenna with wideband characteristics for sub-6 GHz, Ku-band, and millimeter-wave applications, Ain Shams Eng. J. (2023) 102579.
[36] Ahsan Altaf, Amjad Iqbal, Amor Smida, Jamel Smida, Ayman A. Althuwayb, Saad Hassan Kiani, Mohammad Alibakhshikenari, Francisco Falcone, Ernesto Limiti, Isolation improvement in UWB-MIMO antenna system using slotted stub, Electronics 9 (10) (2020) 1582.
[37] Mujeeb Abdullah, Ahsan Altaf, Muhammad Rizwan Anjum, Zulfiqar Ali Arain, Abdul Aleem Jamali, Mohammad Alibakhshikenari, Francisco Falcone, Ernesto Limiti, Future smartphone: MIMO antenna system for 5G mobile terminals, IEEE Access 9 (2021) 91593–91603.
[38] Mehr E. Munir, Saad Hassan Kiani, Huseyin Serif Savci, Mohamed Marey, Jehanzeb Khan, Hala Mostafa, Naser Ojaroudi Parchin, A four element mm-wave MIMO antenna system with wide-band and high isolation characteristics for 5G applications, Micromachines 14 (4) (2023) 776.
[39] Bilal Aghoutane, Sudipta Das, Mohammed E.L. Ghzaoui, B.T.P. Madhav, Hanan El Faylali, A novel dual band high gain 4-port millimeter wave MIMO antenna array for 28/37 GHz 5G applications, AEÜ, Int. J. Electron. Commun. 145 (2022) 154071.